THERMALLY-OPTICALLY-THERMALLY STIMULATED LUMINESCENCE

Dianabasi Akpan[1*], Sunday Ekpo[2], Christopher Effiong[3], Mfoniso Aka[4]

[1,2,3,4]University of Uyo, Uyo*

Corresponding Author:
dianabasiakpan@uniuyo.edu.ng

Abstract

A three-stage energy band model was studied. The model consists of electrons thermally stimulated from the ground state to the first excited state, after which they were optically stimulated into the second excited state and they were finally stimulated thermally into the conduction band. A set of simultaneous differential equations was generated from the models and three assumed conditions were applied to this model, which they were solved analytically and analytical expressions were obtained. The same set of simultaneous equations were solved numerically using ode 15s MATLAB solver. When considering first-order peaks, the kinetic parameters obtained were found to be in good agreement with the analytical expressions. But when considering non first-order peaks, the kinetic parameters obtained numerically were not in good agreement with the analytical expressions and explanations had been given. Second-order peaks could not be obtained despite careful selection of the kinetic parameters because the traps were quickly saturated and the quasi- equilibrium conditions assumed could no longer be satisfied. The stability of the excited TA-OSL signals produced by the model was also studied. The real stability of the excited TA-OSL signals produced by this model was found to be about 46 million years.

1. INTRODUCTION

Thermoluminescence is a process where by materials (natural crystalline minerals like quartz and feldspar) absorb energy from electromagnetic radiation or other ionizing radiation and when subjected to heat release light energy known as luminescence. In some thermoluminescent materials there may be combination of heat and light energies to stimulate them in order to produce luminescence; when this takes place, it is often referred to as thermally-assisted optically stimulated luminescence (TA-OSL). Both thermoluminescence (TL) and optically stimulated luminescence (OSL) have revealed their relevance in dating of anthropological, archaeological, geological specimens and in dosimetry [1-6]. A number of authors had worked on TA-OSL, such authors include: Chen and Pagonis [7]; Chen and Pagonis [8]; Chen and Pagonis [9]; Spooner [10]; Chen and Mckeever [11]; Kalita and Chithambo [12]; Polymeris and George [13] etc. Akpan et al. [14] had worked on a three-stage thermal stimulation of thermoluminescence. In their case only thermal energy at different stages was used to stimulate electrons from a deep trap across the excited states to the conduction band. They based their work on the premise reported by Hutt et al. [15], that the use of infra-red (IR) alone in feldspar to stimulate electron from the deep trap to the conduction band could not be achieved except through the use of thermal assistance. This warranted the electrons to be stimulated thermally through the three stages before reaching the conduction band. Following the same proposition above, this work focuses on a three-stage (thermally-optically-thermally) stimulated luminescence. In this work, the electrons from the deep trap (ground state) are stimulated thermally to the first excited state and as a result of their inability to reach the conduction, they are now stimulated optically to the second excited state. The last stage is the stimulation of electrons thermally from the second excited state into the conduction band.

The aim of this work is to numerically solve the set of simultaneous differential equations generated from the model. The following objectives will be achieved: to obtain different analytical expressions when assumed conditions are applied to the model; determination of effective activation energies and frequency factors numerically; comparison of numerical results with analytical expressions and determination of effective life-time as it affects the stability of TA-OSL signals.

2. MODEL

A three-stage energy band is displayed in fig.1. As the name implies, it consists of three stages namely ground state, first excited state (n_{e1}) and second excited state (n_{e2}). N (cm^3) is the trapping state with concentration; n (cm^3) is the instantaneous occupancy; the activation energy to stimulate the electrons thermally from the ground state into the first excited state is E_1 (eV) and the frequency factor for the ground state is S_1 (s^{-1}). At the first excited state, the electrons can either be retrapped into the ground with a probability of P_1 (s^{-1}) or they can be raised with a stimulating light f (s^{-1}) into the second excited state (n_{e2}). Since the raised electrons cannot reach the conduction band, there is a need for further stimulation from the second excited state to the conduction band. At the second excited state there exists a possibility of the electrons either being retrapped into the first excited state with a probability of P_2 (s^{-1}) or they can be stimulated thermally into the conduction band with an activation energy, E_2 (eV) and the frequency factor, S_2 (s^{-1}). On reaching the conduction band with instantaneous concentration of electrons, n_o (cm^3), the electrons can either be retrapped into the second excited state with retrapping probability coefficient A_n (cm^3s^{-1}), or recombine with a hole in the centre with a recombination probability coefficient A_m (cm^3s^{-1}). It is

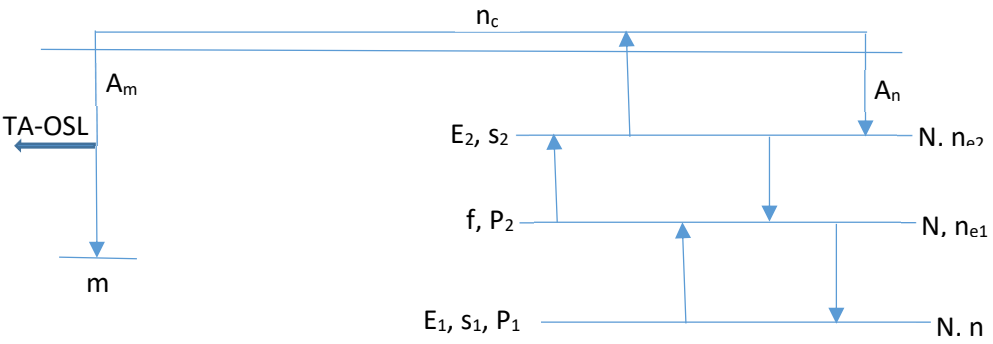

Fig.1: Energy level diagram of a three-stage model

this recombination process that leads to production of TA-OSL photons with an instantaneous intensity I. It must be noted that at the end of initial excitation by irradiation, the number of trapped holes, m_o is equal to the total number of trapped electrons, $n_o + n_{eo1} + n_{eo2} + n_{co}$. Since the initial excitation by irradiation is carried out at relatively low temperature, therefore, n_{eo1}, n_{eo2} and n_{co} are relatively very small compared to n_o, thus number of trapped holes m_o equals the number of trapped electrons (i.e. $m_o \approx n_o$). In this model, we use the detailed-balance principle and neglecting electronic degeneracies as stated by Halperin and Braner [16]: during the first transition, the value of frequency factor must be equal to the value of retrapping probability (i.e. $s_1 = P_1$)

A set of simultaneous differential equations generated from the model during the heating stage:

$$\frac{dn}{dt} = -ns_1 e^{-\frac{E_1}{kT}} + P_1 n_{e1} \quad (1)$$

$$\frac{dn_{e1}}{dt} = ns_1 e^{-\frac{E_1}{kT}} - P_1 n_{e1} - f n_{e1} + P_2 n_{e2} \quad (2)$$

$$\frac{dn_{e2}}{dt} = f n_{e1} - P_2 n_{e2} - s_2 n_{e2} e^{-\frac{E_2}{kT}} + A_n (N - n - n_{e1} - n_{e2}) n_c \quad (3)$$

$$I = -\frac{dm}{dt} = A_m m n_c \quad (4)$$

$$\frac{dn_c}{dt} = \frac{dm}{dt} - \frac{dn}{dt} - \frac{dn_{e1}}{dt} - \frac{dn_{e2}}{dt} \quad (5)$$

3. ANALYTICAL EXPRESSIONS

From eq. (3), we have

$$\frac{dn_{e2}}{dt} + \left(P_2 + s_2 e^{-\frac{E_2}{kT}}\right) n_{e2} = A_n (N - n - n_{e1} - n_{e2}) n_c + f n_{e1} \quad (6)$$

Applying quasi-equilibrium conditions to eq. (6): $\frac{dn_{e2}}{dt} \ll \left(P_2 + s_2 e^{-\frac{E_2}{kT}}\right) n_{e2}$ and $(N - n) \gg (n_{e1} + n_{e2})$

Eq. (6) becomes

$$n_{e2} = \frac{A_n (N-n) n_c + f n_{e1}}{\left(P_2 + S_2 e^{-\frac{E_2}{kT}}\right)} \quad (7)$$

From eq. (2), we have

$$\frac{dn_{e1}}{dt} + (P_1 + f) n_{e1} = ns_1 e^{-\frac{E_1}{kT}} + P_2 n_{e2} \quad (8)$$

But $\frac{dn_{e1}}{dt} \ll (P_1 + f) n_{e1}$

$$n_{e1} = \frac{ns_1 e^{-\frac{E_1}{kT}} + P_2 n_{e2}}{P_2 n_{e2}} \quad (9)$$

Putting eq. (7) into eq. (9)

$$n_{e1} = \frac{P_2 n s_1 e^{-\frac{E_1}{kT}} + n s_1 S_2 e^{-\frac{(E_1+E_2)}{kT}} + P_2 A_n (N-n) n_c}{P_1 P_2 + P_1 S_2 e^{-\frac{E_2}{kT}} + f s_2 e^{-\frac{E_2}{kT}}} \quad (10)$$

Putting eq. (10) into eq. (1), we have

$$\frac{dn}{dt} = -\frac{f s_1 s_2 n e^{-\frac{(E_1+E_2)}{kT}} + P_1 P_2 A_n (N-n) n_c}{P_1 P_2 + (P_1 + f) s_2 e^{-\frac{E_2}{kT}}} \quad (11)$$

$$\frac{dn}{dt} = -s_{eff} n e^{-\frac{(E_1+E_2)}{kT}} + A_{n,eff} (N - n) n_c \quad (12)$$

Where

$$s_{eff} = \frac{f s_1 s_2}{P_1 P_2 + (P_1 + f) s_2 e^{-\frac{E_2}{kT}}} \quad (13)$$

$$A_{n,eff} = \frac{P_1 P_2 A_n}{P_1 P_2 + (P_1 + f) s_2 s_2 e^{-\frac{E_2}{kT}}} \quad (14)$$

For condition 1: $P_1 \gg f$ and $P_2 \gg s_2 e^{-\frac{E_2}{kT}}$

Factorizing eq. (13), we have

$$s_{eff} = \frac{f s_1 s_2}{P_1 P_2 + P_1 s_2 e^{-\frac{E_2}{kT}} + f s_2 e^{-\frac{E_2}{kT}}} \quad (15)$$

If $P_1 \gg f$

$$s_{eff} = \frac{f s_1 s_2}{P_1 P_2 + P_1 s_2 e^{-\frac{E_2}{kT}}} \quad (16)$$

If $P_2 \gg s_2 e^{-\frac{E_2}{kT}}$

$$s_{eff} = \frac{f s_1 s_2}{P_1 P_2} \quad (17)$$

Applying detailed-balance principle, $s_1 = P_1$, therefore eq. (17) becomes

$$s_{eff} = \frac{f s_2}{P_2} \quad (18)$$

Factorizing eq. (14), we have

$$A_{n,eff} = \frac{P_1 P_2 A_n}{P_1 P_2 + P_1 s_2 e^{-\frac{E_2}{kT}} + f s_2 e^{-\frac{E_2}{kT}}} \quad (19)$$

If $P_1 \gg f$

$$A_{n,eff} = \frac{P_2 A_n}{P_2 + s_2 e^{-\frac{E_2}{kT}}} \quad (20)$$

If $P_2 \gg s_2 e^{-\frac{E_2}{kT}}$

$$A_{n,eff} = A_n \quad (21)$$

Putting eqs. (18) and (21) into eq. (12)

$$\frac{dn}{dt} = -\frac{fs_2}{P_2} n e^{-\frac{(E_1+E_2)}{kT}} + A_n(N-n)n_c \quad (22)$$

For condition 2: $P_1 \ll f$ and $P_2 \ll s_2 e^{-\frac{E_2}{kT}}$

If $P_2 \ll s_2 e^{-\frac{E_2}{kT}}$, then eq. (15) becomes

$$s_{eff} = \frac{fs_1}{(P_1+f)e^{-\frac{E_2}{kT}}} \quad (23)$$

If $P_1 \ll f$

$$s_{eff} = s_1 e^{\frac{E_2}{kT}} \quad (24)$$

If $P_2 \ll s_2 e^{-\frac{E_2}{kT}}$, then eq. (19) becomes

$$A_{n,eff} = \frac{P_1 P_2 A_n}{(P_1+f)s_2 e^{-\frac{E_2}{kT}}} \quad (25)$$

If $P_1 \ll f$

$$A_{n,eff} = \frac{P_1 P_2}{fs_2} e^{\frac{E_2}{kT}} A_n \quad (26)$$

Putting eqs. (24) and (26) into eq.(12), we have

$$\frac{dn}{dt} = -s_1 n e^{-\frac{E_1}{kT}} + \frac{P_1 P_2}{fs_2} e^{\frac{E_2}{kT}} A_n(N-n)n_c \quad (27)$$

For condition 3: $P_1 \gg f$ and $P_2 \ll s_2 e^{-\frac{E_2}{kT}}$

If $P_1 \gg f$ then eq. (15) becomes

$$s_{eff} = \frac{fs_2}{P_2+s_2 e^{-\frac{E_2}{kT}}} \quad (28)$$

If $P_2 \ll s_2 e^{-\frac{E_2}{kT}}$ then eq. (28) becomes

$$s_{eff} = f e^{\frac{E_2}{kT}} \quad (29)$$

From eq. (19), if $P_1 \gg f$, then eq. (20) will be obtained.

From eq. (20), if $P_2 \ll s_2 e^{-\frac{E_2}{kT}}$

$$A_{n,eff} = \frac{P_2}{s_2} e^{\frac{E_2}{kT}} A_n \quad (30)$$

Putting eqs. (29) and eq. (31) into eq. (12)

$$\frac{dn}{dt} = -fn e^{-\frac{E_1}{kT}} + \frac{P_2}{s_2} e^{\frac{E_2}{kT}} A_n(N-n)n_c \quad (31)$$

4. NUMERICAL RESULTS

A set of simultaneous equations (1) – (5) was solved numerically for carefully chosen trapping parameters and stimulating light intensity factor f by using ode 15s MATLAB solver. The chosen heating rate β for all the simulations carried out was $1ks^{-1}$.

Fig.2 displays TA-OSL curves simulated using eqs. (1) – (5) for different values of simulating light intensity factors. The trapping parameters used were $E_1 = 0.7eV$; $E_2 = 0.5eV$; $P_1 = s_1 = 10^{16}\ s^{-1}$; $s_2 = 10^{11}s^{-1}$; $A_n = 10^{-12}cm^3s^{-1}$; $A_m = 10^{-7}cm^3s^{-1}$; $P_2 = 10^{14}s^{-1}$, Boltzmann constant $k = 8.617x10^{-5}$ eVk-1; $\beta = 1ks^{-1}$; $N = 1.1x10^{10}cm^{-3}$; $n_o = m_o = 10^{10}cm^{-3}$; $n_{e1o} = n_{e2o} = 0$ and $n_{c0} = 0$. The stimulating light intensity factors were 10^8s^{-1}, $10^{10}s^{-1}$ and $10^{12}s^{-1}$ and these were displayed for curves a, b and c respectively. Each of the glow curves obtained was analyzed by finding the symmetry factor, μ_g, effective activation energy, E_{eff} and effective frequency factor, s_{eff}. These parameters were found by using the formulae expressed by Chen [17]. The formulae are:

1. For the symmetry factory, μ_g

$$\mu_g = \frac{\delta}{\omega} \quad (32)$$

Where $\delta = T_2 - T_m$ and $\omega = T_2 - T_1$; T_1 is the low temperature of half intensity; T_2 is the high temperature of half intensity and T_m is the temperature at maximum intensity. When $\mu_g = 0.42$, the glow peak is a typical first-order peak and when $\mu_g \approx 0.52$ the glow peak is a typical second-order peak.

2. Activation energy, E_{eff} for first-order peak was calculated using:

$$E_{eff} = KT_m(2.52\frac{T_m}{\omega} - 2) \quad (33)$$

3. Activation energy, E_{eff} for second-order peak was calculated using:

$$E_{eff} = KT_m(3.54\frac{T_m}{\omega} - 2) \quad (34)$$

4. For frequency factor, s, we used

$$s = \frac{\beta E}{KT^2{}_m}\exp(\frac{\beta E}{KT^2{}_m})\ [1 + (b-1)\frac{2kT_m}{E}]^{-1} \quad (35)$$

Where E is the activation energy and b is order of kinetics. Other parameters have their usual meaning as earlier stated above.

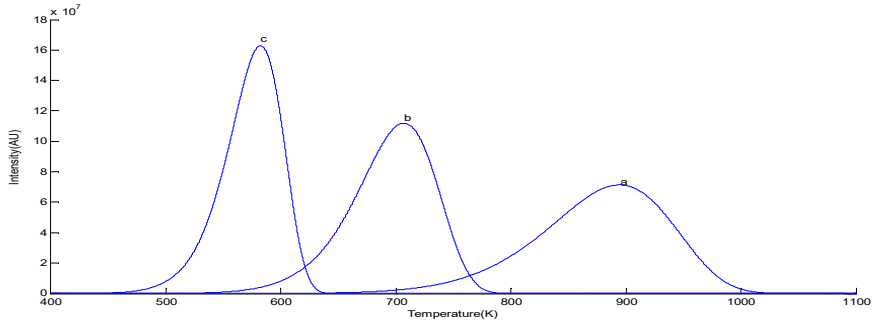

Fig. 2: Simulated results of TA-OSL peaks using eqs. (1) - (5). The trapping parameters used are $E_1 = 0.7$eV; $E_2 = 0.5$eV; $P_1 = s_1 = 10^{16}$ s^{-1}; $s_2 = 10^{11}$s^{-1}; $A_n = 10^{-12}$cm^{3}s^{-1}; $A_m = 10^{-7}$cm^{3}s^{-1}; $P_2 = 10^{14}$s^{-1}; $\beta = 1$ks^{-1}; $N = 1.1\text{x}10^{10}$cm^{-3}; $n_o = m_o = 10^{10}$cm^{-3}; $n_{e1o} = n_{e2o} = 0$ and $n_{c0} = 0$. The stimulating light intensity factors for curves 'a', 'b' and 'c' are f = 10^8s^{-1}, f = 10^{10}s^{-1} and f = 10^{12}s^{-1} respectively.

From fig.2, curve a, the peak shape was like a typical first-order TL peak with symmetry factor, ≈ 0.43. Its effective activation energy, E_{eff} calculated using eq. (33) was 1.20eV and effective frequency factor, s_{eff} calculated using eq. (35) was 1.00 x 10^5s^{-1}. For curve b, the symmetry, effective activation energy and effective frequency factor were 0.43, 1.20eV and 1.00 x 10^7s^{-1} respectively. For curve c, the symmetry factor, effective activation energy and effective frequency factor were 0.42, 1.20eV and 1.00 x 10^9s^{-1} respectively.

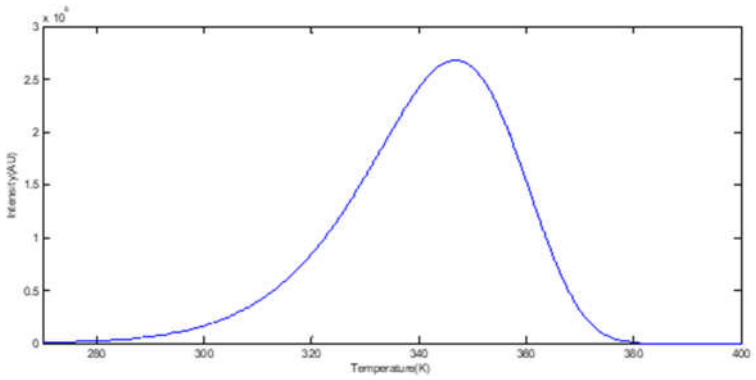

Fig.3: Simulated result of TA-OSL peak using eqs. (1) - (5). It uses the same trapping parameters as in fig. 2 except that $P_1 = s_1 = 10^9$s^{-1}, $s_2 = 10^{14}$s^{-1} and f = 10^{13}s^{-1}.

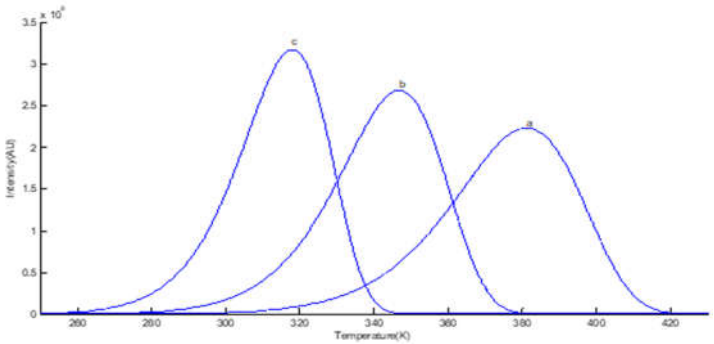

Fig. 4: Simulated results of TA-OSL peaks using eqs. (1) - (5). It uses the same trapping parameters as in fig. 3 except that $P_1 = s_1 = 10^{13}$s^{-1} and f = 10^8s^{-1}, 10^9s^{-1} and 10^{10}s^{-1}. The stimulating light intensity factors for curves 'a', 'b' and 'c' are f = 10^8s^{-1}, f = 10^9s^{-1} and f = 10^{10}s^{-1}are respectively.

Fig.3 uses the same trapping parameters as in fig.2 except that $P_1 = s_1 = 10^9 s^{-1}$, $s_2 = 10^{14} s^{-1}$ and $f = 10^{13} s^{-1}$. The obtained peak is like a typical first-order TL peak with symmetry factor, $\mu_g \approx 0.42$. The effective activation energy, E_{eff} and effective frequency factor, s_{eff} were 0.70eV and 1.00 x $10^9 s^{-1}$ respectively.

Fig.4 uses the same trapping parameters as in fig.3 except that $P_1 = s_1 = 10^{13} s^{-1}$ and $f = 10^8 s^{-1}$, $10^9 s^{-1}$ and $10^{10} s^{-1}$. TA-OSL curves 'a', 'b' and 'c' represented the stimulating light factors for $f = 10^8 s^{-1}$, $10^9 s^{-1}$ and $10^{10} s^{-1}$ respectively. The symmetry factors for all the three curves were the same ($\mu_g \approx 0.42$). The effective activation energies for curves 'a', 'b' and 'c' were 0.70eV, 0.70eV and 0.71eV respectively. The effective frequency factors for curves 'a', 'b' and 'c' were 1.00 x $10^8 s^{-1}$, 1.00 x $10^9 s^{-1}$ and 1.46 x $10^{10} s^{-1}$ respectively.

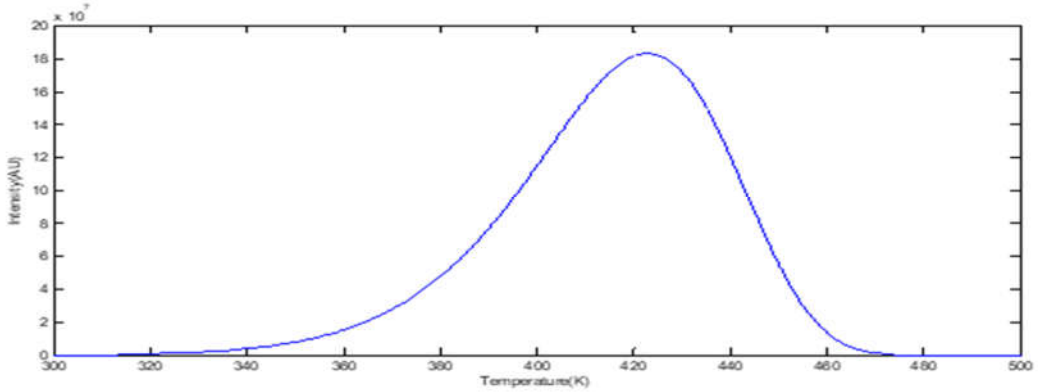

Fig.5: Simulated results of TA-OSL peaks using eqs. (1) - (5). It uses the same trapping parameters as in fig. 2 except that $E_2 = 0$eV and $f = 10^{10} s^{-1}$.

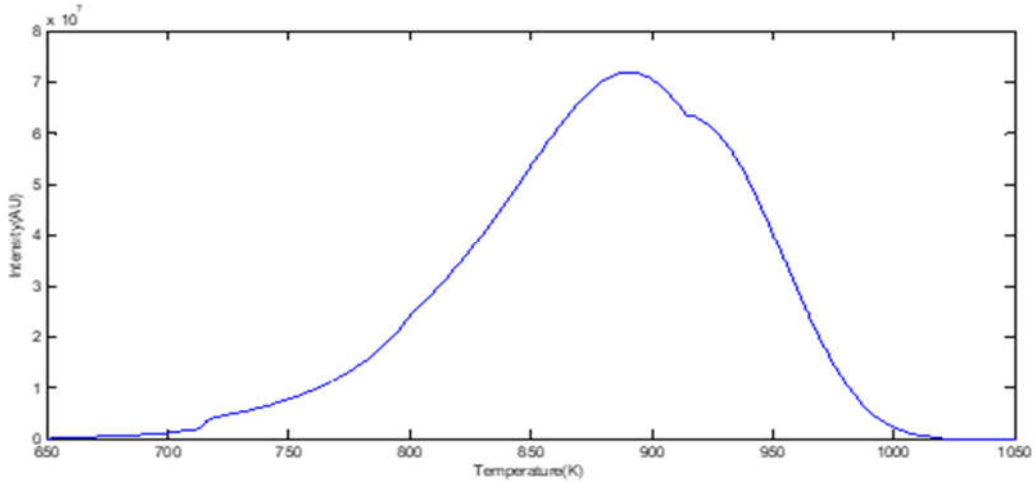

Fig.6: Simulated results of TA-OSL peaks using eqs. (1) - (5). It uses the same trapping parameters as in fig. 2 except that $A_n = 10^{-11} cm^3 s^{-1}$, $A_m = 10^{-14} cm^3 s^{-1}$ and $f = 10^{10} s^{-1}$. This is TA-OSL glow curve with an intermediate geometrical symmetry factor, $\mu_g \approx 0.48$

Fig.5 uses the same kinetic parameters as in fig.2 except that $E_2 = 0$eV and $f = 10^{10} s^{-1}$. The peak obtained was like a typical first order TL peak with $\mu_g \approx 0.43$. Using eq. (33) to evaluate, $E_{eff} \approx 0.70$ eV and using eq. (35) to evaluate, $s_{eff} \approx 1.00 \times 10^7 s^{-1}$.

A glow curve with an intermediate geometrical factor ($\mu_g \approx 0.43$) is displayed in fig.6. The simulated TA-OSL curve in fig.6 uses the same trapping parameters as in fig. 2 except that $A_n = 10^{-11} cm^3 s^{-1}$, $A_m = 10^{-14} cm^3 s^{-1}$ and $f = 10^{10} s^{-1}$. Using eqs. (33) and (35) to calculate the kinetic parameters, $E_{eff} \approx 1.16$eV and $s_{eff} \approx 0.62 \times 10^5 s^{-1}$ were obtained respectively. But when using eqs. (34) and (35) to calculate the kinetic parameters, $E_{eff} \approx 1.69$eV and $s_{eff} \approx 0.90 \times 10^8 s^{-1}$ were obtained respectively.

5. DISCUSSION

The trapping parameters simulated numerically from curve 'a' in fig.2 were $E_{eff} \approx 1.20$eV and $s_{eff} \approx 1.00 \times 10^5 s^{-1}$. Three assumed conditions were applied to this model analytically. The trapping parameters were carefully chosen to meet condition 1: $p_1 >> f$ and $p_2 >> s_2 \exp(-E_2/kT)$. Using eq. (18) to evaluate s_{eff} analytically, then $s_{eff} \approx 1.00 \times 10^5 s^{-1}$. From eq. (22), we see that $E_{eff} \approx E_1 + E_2$ i.e. $E_{eff} = (0.7 + 0.5)$ eV = 1.20eV. It is observed that the numerical results were in good agreement with the analytical results. For curve 'b' in fig.2, the numerical results were $E_{eff} \approx 1.20$eV and $s_{eff} \approx 1.00 \times 10^7 s^{-1}$ and for curve 'c' in fig2, the numerical results were $E_{eff} \approx 1.20$eV and $s_{eff} \approx 1.00 \times 10^9 s^{-1}$. The kinetic trapping parameters obtained analytically as applied to condition 1 from curves 'a', 'b' and 'c' were found to be in very good agreement with the numerical results.

In fig.3, the trapping parameters obtained numerically were $E_{eff} \approx 0.70$eV and $s_{eff} \approx 1.00 \times 10^{9} s^{-1}$. The kinetic parameters were carefully chosen to meet condition 2 before simulation was carried out. From eq. (27) (that is the left hand side), the electrons were majorly stimulated thermally by E_1. Therefore, E_{eff} was reduced from '$E_1 + E_2$ to E_1. The reason for the reduction in the effective activation was as a result of the exponential temperature dependence on s_{eff} (see eq. (24)). Akpan et al. [14] and Chen et al. [18] observed exponential temperature dependence on s_{eff} which caused reduction in the activation energies. From Akpan et al. [14], E_{eff} was reduced from '$E_1 + E_2 + E_3$' to '$E_1 + E_2$' as seen in their eq. (28) and from Chen et al. [18], E_{eff} was reduced from '$E_1 + E_2$' to 'E_1' as seen in their eq. (15). Therefore, it can be established that whenever there is an exponential dependence on s_{eff}, there will be reduction in the effective activation energy (E_{eff}). However, despite the reduction in the E_{eff}, the numerical results obtained in fig.3 were found to be in good agreement with the analytical expressions.

The symmetry factors for curves 'a', 'b' and 'c' in fig.4 obtained were typical first-order TL peak with the same $\mu_g \approx 0.42$. The E_{effs} obtained for curves 'a', 'b' and 'c' were 0.70eV, 0.70eV and 0.71eV respectively. From eq. (31), E_{eff} was reduced from '$E_1 + E_2$' to 'E_1'. The reason for this reduction in E_{eff} was that s_{eff} was dependent on the exponential temperature as seen in eq. (29) and this was earlier explained. The kinetic parameters (E_{eff} and s_{eff}) obtained numerically were found to be in constant with the analytical results.

We examined a condition in which the second excited state is cut off i.e. ($E_2 = 0$). In this case the electrons were not thermally excited into the condition band but optically stimulated into the conduction band. The TA-OSL glow curve is shown in fig.5. The model now reduces to a two-stage stimulation whereby in the first stage, the electrons are thermally stimulated from the ground state to the first excited state. In the second stage, the electrons are stimulated optically into the conduction band. This was one of the models simulated by Chen and Pagonis [7]. Analyzing the glow curve in fig. 5, E_{eff} was approximately 0.70eV and s_{eff} was about $1.00 \times 10^{7} s^{-1}$. The kinetic parameters obtained numerically were found to be in harmony with the analytical results. It must be noted that by making $E_1 = 0$, no TA-OSL photons will be produced because at the ground state, the deep trapped electrons cannot be stimulated into the first excited state. Consequently, no TA-OSL glow curve will be produced, hence numerical results will not be obtained.

In our present model one does not need to emphasize on the importance of stimulating light intensity factor. If the stimulating intensity light factor becomes zero ($f = 0$), no TA-OSL photon is produced. This is because thermally-assisted optically-stimulated luminescence is strongly dependent on the optical light. From eq. (13), if $f = 0$, the effective frequency factor can never be obtained. Moreover, when $f = 0$, the first term on the right of eq. (22) becomes zero and since the second term on the right of eq. (22) is always very small (negligible), therefore TA-OSL photons cannot be produced.

Fig.6 shows TA-OSL glow curve with $\mu_g \approx 0.48$. This is a glow curve with an intermediate geometrical symmetry factor. Using eqs. (33) and (35) to calculate its kinetic parameters, we had $E_{eff} \approx 1.16$eV and $s_{eff} \approx 0.62 \times 10^{5} s^{-1}$. Considering the effective activation energy, the numerical result was found to be in good agreement with analytical expression. But considering effective frequency factor, the numerical result was found to be in variance with analytical expression. Then using eqs. (34) and (35), we had $E_{eff} \approx 1.69$eV and $s_{eff} \approx 0.90 \times 10^{8} s^{-1}$. In this case considering E_{eff}, the numerical result was found not to be in good agreement with analytical expression while for s_{eff}, the numerical result was close to the analytical result obtained. The reason for these discrepancies in results is using first and second kinetic formulae to calculate for kinetic parameters of an intermediate glow curve.

There are certain principles that must be followed for first and second order glow curves to be obtained. According to Randall and Wilkins [19] if the recombination probability coefficient is greater than the retrapping probability coefficient, the glow curve obtain would be a narrow peak shape. According to Garlick and Gibson [20] if the retrapping probability coefficient is greater than the recombination probability coefficient, the glow curve obtain would be a wide peak. In our model, when the retrapping probability coefficient was greater than recombination probability coefficient (even to 5 orders) obtaining a glow curve in which its geometrical symmetry factor was second order was not possible. The reason for this is not far-fetched. When $A_n >> A_m$, initially more of the electrons will be retrapped and there after the trap becomes saturated. When this happens the quasi-equilibrium conditions assumed can no longer be satisfied. Therefore $N = n$ and $m \neq n$, more electrons will be found at the conduction band since retrapping does not occur again and many electrons recombine with holes at the centre to form TA-OSL photons. Consequently A_m becomes far greater than A_n and TA-OSL curve obtained is like first-order peak.

The stability of a given glow peak is strongly dependent on the temperature at which the sample is held following excitation prior to heating provided the heating does not start immediately after excitation [21]. In order to evaluate the stability of TA-OSL signal, a formular given by Wintle [22] was used. Effective life-time is given as

$$\tau_{eff} = \left(\frac{1}{s_{eff}}\right)\exp\left(\frac{E_{eff}}{kT}\right) \quad (36)$$

Where s_{eff} is the effective frequency factor; E_{eff} is the effective activation energy, k is the Boltzmann constant; τ_{eff} is the effective life-time and T is the room temperature (300k).

From fig.2 (curve 'a'), the obtained kinetic parameters were $E_{eff} \approx 1.20$eV and $s_{eff} \approx 1.00 \times 10^5 s^{-1}$. Using eq. (36) to calculate, we have $\tau_{eff} \approx 1.45 \times 10^{15}$s i.e. about 45.8×10^6 years. From fig.6, the obtained kinetic parameters were: (i) $E_{eff} \approx 1.16$eV and $s_{eff} \approx 0.62 \times 10^5 s^{-1}$ which gave $\tau_{eff} \approx 4.96 \times 10^{14}$s i.e. about 15.73×10^6 years. (ii) $E_{eff} \approx 1.69$eV and $s_{eff} \approx 0.90 \times 10^8 s^{-1}$ which gave $\tau_{eff} \approx 2.74 \times 10^8$s i.e. about 8.69×10^{12} years. The life-time of the TA-OSL signal calculated from fig.6 are anomalous stability since they are calculated from non-first order peaks. One may think that the life-time of the excited TA-OSL signal is very stable for about a period of about 8,960 billion years. Pure first-order peak will produce meaningful life-time of the excited state and non-first order cases may not yield the desired results [9]. Therefore, the real life-time of TA-OSL signal of this model is about 46 million years. The great disparity observed between the real life-time and anomalous life-time of the excited TA-OSL signal is as a result of the different effective activation energies and frequency factors obtained.

6. CONCLUSION

A three-stage energy band model has been studied. The electrons were stimulated thermally from the ground state to the first excited state. After which they were optically raised from the first excited state into the second excited state. Then electrons were finally raised thermally into the conduction band where they can either be retrapped into the second excited state or recombine with holes at the centre to produce TA-OSL photons. When considering the first-order peaks, numerical results were found to be in good agreement with the analytical expressions. But when considering a non-first order peaks, the numerical results were in variance with the analytical results the analytical results. The reasons for these variations were given. The real stability of excited signal produced by the three-stage energy band model was found to be about 46 million years.

REFERENCES

[1]. E. Bulur, "An alternative technique for optically stimulated luminescence," in Radiat. Meas. 26, 701-709, 1996.
[2]. D.J. Huntley, D.I. Godfrey-Smith, & M.L.W. Thewalt, "Optical dating of sediments," in Nature 313, 105-107, 1985.
[3]. S.W.S. McKeever, "Thermoluminescence of solids," Cambridge University Press, USA, PP.374, 1985.
[4]. R. Chen, "Theory of thermoluminescence and related phenomena," in World Scientific Publishing Co. Pvt. Ltd.
[5]. M. Zahedifar, S. Harooni & E. Sadeghi, "Thermoluminescence kinetic analysis of quartz using an improved general mode for exponential distribution of activation energies," in Nuccl. Instrum. Methods A 654, 569 – 574, 2011.
[6]. N. D. Sang, "Estimate half-life of thermoluminescence signals according to the different models by using Python," in Journal of Taibah University for science. 15 (1), 599-608, 2021.
[7]. R. Chen, & V. Pagonis, "Modeling TL-like thermally assisted optically stimulated luminescence (TA-OSL)," in Radiat. Meas.56, 6-12, 2013.
[8]. R. Chen, & V. Pagonis, "The role of simulations in the study of thermoluminescence (TL)," Radiat. Meas. 1-7, 2014.
[9]. R. Chen, & V. Pagonis, "Study of the stability of the TL and OSL signals," Radiat. Meas. 81, 192-197, 2015.
[10]. N. A. Spooner, "The anomalous fading of infrared-stimulated luminescence from feldspars," Radiat. Meas. 23, 625-632, 1994.
[11]. R. Chen & S.W.S. Mckeever, "Theory of thermoluminescence and related phenomena," in World Scientific, Singapore. Pages 1-146, 1997.
[12]. J. M. Kalita & M. L. Chithambo, "Themoluminescence of α-Al_20_3:C,Mg: Kinetic analysis of the main glow peak," Journal of Luminescence 182, 177-182, 2017.
[13]. G. S. Polymeris & K. George, "Advances in physics and applications of optically and thermally stimulated luminescence," Pages 131-171, 2019.
[14]. D. Akpan, A. Ekanem, & B. Ebiang, "A Three-stage thermal Stimulation of thermoluminescence (TL)," in Journal of Luminescence and Applications. 4(1), 10-29, 2017.
[15]. G. Hutt, I. Jaek & J. Tchonka, "Optical dating: k-feldspars optical response stimulation spectra," in Quarter. Sci. Rev. 7, 381-385, 1988.
[16]. A. Halperin & A.A. Braner, "Evaluation of thermal activation energies from glow curves," in Physiol. Rev. 117, 408-415, 1960.
[17]. R. Chen, "On the calculation of activation energies and frequency factors from glow curves," in J. Appl. Phys. 40, 570-585, 1969.
[18]. R. Chen, J.L. Lawless & V. Pagonis, "Two-stage thermal stimulation of thermoluminescence," in Radiat. Meas. 47, 809-813, 2012.
[19]. J. T. Randall & M. H. F. Wilkins, "Phosphorescence and electron traps.The study of traps distributions," in Proc. Roy. Soc. Lond. A 184, 366, 1945.
[20]. G. F.J. Garlick & A. F. Gibson, "The electron trap mechanism of luminescence in sulphide and silicate phosphors," in Proc. Phys. Soc. 60, 574, 1948.
[21]. J. L. Lawless, R. Chen & V. Pagonis, "A model for explaining the inability of exciting thermoluminescence (TL) peaks in certain low temperature ranges," in Radiat. Meas. 145, 106610, 2021.
[22]. A.G. Wintle, "Thermal quenching of thermoluminescence in quartz," in Geophys. J.R. Astr. Soc. 41, 107-113, 1975.